Title

Preclinical assessment of MEK1/2 inhibitors for neurofibromatosis type 2–associated schwannomas reveals differences in efficacy and drug resistance development

Journal

Neuro-Oncology, 21(4)

ISSN

1522-8517

Authors

Fuse, Marisa A
Dinh, Christine T
Vitte, Jeremie
et al.

Publication Date

2019-03-18

DOI

10.1093/neuonc/noz002

Peer reviewed

Neuro-Oncology
21(4), 486–497, 2019 | doi:10.1093/neuonc/noz002 | Advance Access date 6 January 2019

Preclinical assessment of MEK1/2 inhibitors for neurofibromatosis type 2–associated schwannomas reveals differences in efficacy and drug resistance development

Marisa A. Fuse, Christine T. Dinh, Jeremie Vitte, Joanna Kirkpatrick, Thomas Mindos, Stephani Klingeman Plati, Juan I. Young, Jie Huang, Annemarie Carlstedt, Maria Clara Franco, Konstantin Brnjos, Jackson Nagamoto, Alejandra M. Petrilli, Alicja J. Copik, Julia N. Soulakova, Olena Bracho, Denise Yan, Rahul Mittal, Rulong Shen, Fred F. Telischi, Helen Morrison, Marco Giovannini, Xue-Zhong Liu, Long-Sheng Chang, and Cristina Fernandez-Valle

Burnett School of Biomedical Sciences, College of Medicine, University of Central Florida (UCF), Orlando, Florida, USA (M.A.F., S.K.P., M.C.F., K.B., J.N., A.P., A.J.C., J.N.S., C.F-V.); Department of Otolaryngology, University of Miami Miller School of Medicine, Miami, Florida, USA (C.T.D., O.B., D.Y., R.M., F.F.T., X.Z-L.); Department of Head and Neck Surgery, David Geffen School of Medicine at UCLA and Jonsson Comprehensive Cancer Center, University of California at Los Angeles (UCLA), Los Angeles, California, USA (J.V., M.G.); Leibniz Institute on Aging, Fritz Lipmann Institute, Jena, Germany (J.K., T.M., A.C., H.M.); Department of Human Genetics, University of Miami Miller School of Medicine, Miami, Florida, USA (J.I.Y., X.-Z.L.); Center for Childhood Cancer and Blood Diseases, Nationwide Children's Hospital (J.H., L-S.C.) and Departments of Pediatrics (J.H., L.-S.C.) and Pathology, The Ohio State University (R.S.), Columbus, Ohio, USA

Corresponding Author: Cristina Fernandez-Valle, Ph.D., Burnett School of Biomedical Sciences, College of Medicine, University of Central Florida, 6900 Lake Nona Blvd, Orlando, FL 32827 (cfv@ucf.edu).

Abstract

Background. Neurofibromatosis type 2 (NF2) is a genetic tumor-predisposition disorder caused by *NF2*/merlin tumor suppressor gene inactivation. The hallmark of NF2 is formation of bilateral vestibular schwannomas (VS). Because merlin modulates activity of the Ras/Raf/mitogen-activated protein kinase kinase (MEK)/extracellular signal-regulated kinase (ERK) pathway, we investigated repurposing drugs targeting MEK1 and/or MEK2 as a treatment for NF2-associated schwannomas.

Methods. Mouse and human merlin-deficient Schwann cell lines (MD-MSC/HSC) were screened against 6 MEK1/2 inhibitors. Efficacious drugs were tested in orthotopic allograft and *NF2* transgenic mouse models. Pathway and proteome analyses were conducted. Drug efficacy was examined in primary human VS cells with *NF2* mutations and correlated with DNA methylation patterns.

Results. Trametinib, PD0325901, and cobimetinib were most effective in reducing MD-MSC/HSC viability. Each decreased phosphorylated pERK1/2 and cyclin D1, increased p27, and induced caspase-3 cleavage in MD-MSCs. Proteomic analysis confirmed cell cycle arrest and activation of pro-apoptotic pathways in trametinib-treated MD-MSCs. The 3 inhibitors slowed allograft growth; however, decreased pERK1/2, cyclin D1, and Ki-67 levels were observed only in PD0325901 and cobimetinib-treated grafts. Tumor burden and average tumor size were reduced in trametinib-treated *NF2* transgenic mice; however, tumors did not exhibit reduced pERK1/2 levels. Trametinib and PD0325901 modestly reduced viability of several primary human VS cell cultures with *NF2* mutations. DNA methylation analysis of PD0325901-resistant versus -susceptible VS identified genes that could contribute to drug resistance.

Conclusion. MEK inhibitors exhibited differences in antitumor efficacy resistance in schwannoma models with possible emergence of trametinib resistance. The results support further investigation of MEK inhibitors in combination with other targeted drugs for NF2 schwannomas.

Key Points

1. Cobimetinib and trametinib reduced NF2 schwannoma model cell proliferation in vitro and in vivo.
2. Biochemical/proteome analyses reveal cell cycle arrest and apoptosis of trametinib-treated cells.
3. Human vestibular schwannoma cell viability is modestly inhibited by PD0325901 and trametinib.

Importance of the Study

There are currently no FDA-approved drug therapies for the treatment of NF2-associated schwannomas. Clinical trials for selumetinib and cobimetinib are ongoing for assessment of efficacy for NF2-associated tumors and hearing loss; however, little preclinical data have been published. Here, we evaluated 6 MEK1/2 inhibitors for efficacy in mouse and human cell and animal models as well as patient-derived vestibular schwannoma cells with *NF2* mutations. We observed differences in efficacy among the inhibitors as well as the possibility of drug resistance development. Our work highlights the importance of comprehensive drug screening in multiple model systems and supports further investigation of MEK inhibitors alone and in combination with other targeted therapies.

Neurofibromatosis type 2 (NF2) is caused by mutations in the *NF2* gene encoding the merlin tumor suppressor.[1,2] NF2 patients classically present with bilateral vestibular schwannomas (VS) involving the cochleovestibular nerves important for hearing and balance, and can develop additional peripheral schwannomas, meningiomas, and ependymomas.[3] Management of NF2 requires a complex, multidisciplinary approach focused on balancing tumor control and nerve function preservation to improve quality of life and maximize survival.[4] Whereas microsurgical resection of tumors risks permanent nerve injury, radiation therapy increases the chance of malignant transformation of benign tumors and secondary malignancies.[5–10] Therefore, there is an ongoing search for effective drug therapies for NF2.

Schwann cells with loss of merlin tumor suppressor function have elevated levels of Ras/Raf/mitogen-activated protein kinase kinase (MEK)/extracellular signal-regulated kinase (ERK) signaling that promotes cell proliferation.[11–13] Sixteen small molecule MEK inhibitors have entered clinical trials for various cancers.[14] Among these MEK inhibitors, selumetinib (AZD6244) was recently granted Orphan Drug Designation by the FDA for treatment of inoperable plexiform neurofibromas in children with NF1.[15] Additionally, selumetinib reduced growth of an in vitro human schwannoma model.[16,17] This success has prompted additional trials of selumetinib for NF1 and NF2 (NCT numbers: 01089101, 01362803, 02839720, 03259633, 03095248).

Trametinib (Mekinist, GSK1120212, JTP-74057, GlaxoSmithKline) is an allosteric, second-generation, adenosine triphosphate non-competitive reversible MEK1/2 inhibitor that also blocks Raf-dependent phosphorylation of MEK Ser218.[14] Trametinib promotes cell cycle arrest and caspase cleavage in cultured colorectal cells, and demonstrates more potent antitumor activity than other second-generation MEK inhibitors, PD0325901 and selumetinib. It is FDA approved for metastatic melanoma and is in phase I clinical trial for NF1-associated plexiform neurofibromas (NCT02124772).[18]

PD0325901 (Pfizer) is also an allosteric MEK1/2 inhibitor and is a synthetic analog of the first-generation MEK1/2 inhibitor, CI-1040.[14,19] In an *Nf1* genetically engineered mouse model, PD0325901 prolonged survival of mice with malignant peripheral nerve sheath tumors and decreased neurofibroma size in over 80% of mice.[20] Tumor regrowth was observed when treatment was suspended.[21] A phase II open-label study is ongoing for PD0325901 in NF1 (NCT02096471).[14]

Cobimetinib (XL518, GDC-0973, Cotellic, Exelixis/Genentech) is derived from methanone and was FDA approved in 2015 for use in combination with vemurafenib, a BRAF inhibitor, for advanced melanoma with *BRAF* mutations.[22,23] Cobimetinib inhibited growth of tumors with *BRAF* and *KRAS* mutations in xenograft models.[24–26] Phase I studies of cobimetinib for solid tumors reported a manageable toxicity profile with signs of efficacy in tumors with $BRAF^{V600E}$ mutations.[27] Cobimetinib is in clinical trial for pediatric and young adult patients with rasopathies, including NF2 (NCT02639546), treated previously for solid tumors.

Here, we used mouse and human merlin-deficient Schwann cell lines (MD-MSC/HSC) and animal models to evaluate the growth-inhibitory and antitumor activities of a panel of MEK inhibitors. Also, we assessed their efficacy in primary human VS with NF2 mutations.

Materials and Methods

Cell Culture

Wild-type (WT)-MSCs and MD-MSCs were generated and characterized in 2010.[28] MD-MSCs were transduced with lentiviral luciferase as previously reported.[29] MD-schwannoma (MD-SCN) cells were derived from paraspinal schwannomas of *Periostin-Cre*:*Nf2*$^{flox2/flox2}$ mice with *Nf2* inactivation (provided by Dr Wade Clapp, Indiana University). Human Schwann cells (HSCs) were purchased from ScienCell Research Laboratories (catalog #1700, lot #7228), and the generation of a merlin-deficient HSC (MD-HSC) line using lentiviral short hairpin (sh)RNA targeting *NF2* (Sigma Mission, SHCLNV-TRCN0000237845) was previously described.[30] Cells were tested monthly for *Mycoplasma* contamination (Lookout *Mycoplasma* PCR Detection Kit, Sigma).

Mouse Model Systems

NSG (*NOD.Cg-Prkdcscid Il2rgtmlWjl/SzJ*) mice were used at 6–10 weeks of age. *P0-SCH-Δ(39–121)-27* transgenic mice[31] in the BALB/c background were used as a genetically engineered mouse (GEM) model of NF2 schwannomas. Animal use was approved by the Institutional Animal Care and Usage Committees of UCF and UCLA, and the Animal Care and Use Review Office of the United States Army Medical Research and Materiel Command.

Human VS Samples

Through an institutional review board (IRB) approved protocol, the University of Miami Tissue Bank Core Facility (UM-TBCF) consented patients undergoing surgery for brain tumors to harvest samples for research purposes. De-identified fresh human VS were obtained from UM-TBCF through an IRB-exempt protocol. Primary VS cells were prepared and cultured as previously reported.[29,30]

Drug Formulations

MEK inhibitors were purchased from MedChemExpress. Drugs were prepared in dimethyl sulfoxide (DMSO) (stock 10 mM) and diluted to final concentrations in cell culture medium for in vitro work. For animal studies, drugs were solubilized in DMSO at 50–100 mg/mL and diluted in 0.1 M citrate buffer (pH 3) for oral dosing.

Cell Viability Assays

Cells were seeded in 384-well CellBind plates (Corning) at 2000–2500 cells/well in phenol red-free growth medium. WT-MSCs were seeded at 15 000 cells/well in 96-well plates coated with poly-L-lysine (200 μg/mL) and laminin (25 μg/mL). Attached cells were treated with drug or DMSO for 48 h (mouse) or 72 h (human); viability was measured with the CellTiter-Fluor Assay (Promega). Primary human VS cells were seeded (passage 1 or 2) in 96-well plates at 10 000 cells/well. After 24 hours, cells were treated with drug or DMSO for 72 h. Crystal violet assay was performed using a SpectraMax 190 microplate reader (Molecular Devices) to assess cell number, as previously described.[29,30]

Membrane Asymmetry Assay

MD-MSCs were grown at 200 000 cells/well in 12-well CellBind plates (Corning). When at ~80% confluency, cells were treated with drug for 18–24 h, then harvested with 0.05% trypsin and resuspended in Hanks Balanced Salt Solution. The Violet Ratiometric Membrane Asymmetry Assay (Invitrogen) was used to detect apoptosis per the manufacturer's instructions. Cell populations were measured by flow cytometry (Cytoflex, Beckman Coulter) and analyzed with CytExpert software (Beckman Coulter).

Mouse Studies

For pharmacokinetic analysis, at each timepoint 3 mice received drug (1 mg/kg trametinib, 1.5 mg/kg PD0325901, or 20 mg/kg cobimetinib); one mouse received vehicle alone (0.1 M citrate, pH 3, 2% DMSO). Mice were sacrificed after 0.5–32 h; blood and sciatic nerve samples were collected and analyzed by mass spectrometry at Sanford Burnham Prebys Medical Discovery Institute (Lake Nona, Florida).

The orthotopic allograft model using luciferase-expressing MD-MSCs was generated as previously described.[29] Upon confirmation of successful grafting, mice were randomized into treatment groups and received drug or vehicle at the above concentrations daily by oral gavage. Mice were imaged weekly for bioluminescence using the In Vivo Imaging System (IVIS, Caliper) or Bruker MI Imaging System. After 13–14 days of treatment, mice were sacrificed; grafts and contralateral sciatic nerves were removed, weighed, and photographed. Grafts were fixed overnight in 4% paraformaldehyde and stored in 30% sucrose (0.02% azide in phosphate buffered saline) at 4°C. List of antibodies used is provided in Supplementary Methods.

Four-week-old *P0-SCH-Δ(39–121)-27* transgenic mice[31] were treated daily with trametinib (1 mg/kg) or vehicle (0.1 M citrate buffer pH 3, 0.2% DMSO) by oral gavage for 8 weeks. Spinal nerve roots were histopathologically scored at the endpoint as previously described.[32] Following a blind procedure, measurements of tumors and nerve root areas were performed using Zeiss Axiovision software on hematoxylin and eosin stained parasagittal sections of cervical, thoracic, lumbar, and sacral spinal cord segments. The total area of nerve root analyzed was comparable between the trametinib and vehicle-treated groups ($P = 0.1541$).

Western Blotting

Western blots were performed as previously described.[29] Protein was extracted from human VS tumors using radioimmunoprecipitation buffer with protease and phosphatase inhibitors (ThermoFisher). Human VS blots were blocked in 3% bovine serum albumin and incubated

overnight in primary antibody solution at 4°C, followed by incubation with Alexa Fluor 488 and 647 conjugated secondary antibodies (1:200; ThermoFisher) for 2 hours at room temperature and imaged using the ImageQuant LAS 4000 Imager (GE Healthcare).

NF2 Mutation Analysis

Total DNA was extracted from fresh tumor tissues using the QIAamp DNA Mini Kit (Qiagen) and purified using the QIAquick PCR Purification Kit (Qiagen). All VS were tested for mutations within the NF2 gene with multiplex ligation-dependent probe amplification using the Salsa MLPA NF2 Kit (MRC-Holland) per the manufacturer's instructions. Copy number alterations in all 17 exons of the NF2 gene (NM_000268.3) were analyzed with Coffalyser. Additional details are provided in the Supplementary Methods.

DNA Methylation Analysis

High-throughput DNA methylation analysis was performed for 7 human VS tumors using the Infinium MethylationEPIC Kit (Illumina) according to the manufacturer's instructions. Methylation patterns were compared between VS that had a statistically significant decrease in cell number following a 72 hour incubation with 3 μM PD0325901 and those with no response. Additional details are provided in Supplementary Methods.

Proteome

Protein from cell pellets of MD-MSCs treated with trametinib or vehicle was extracted, denatured and prepared for liquid chromatography–tandem mass spectrometry (LC-MS/MS) as described in the Supplementary Methods. MS/MS spectra were searched against the *Mus Musculus* Swiss-Prot entries of the Uniprot KB (database release 2016_01, 16755 entries) using the Andromeda search engine.[33] The specific search criteria and analytics used are provided in Supplementary Methods. Protein differential expression between the trametinib and vehicle control samples was evaluated using the Limma package.[34]

Statistics

Using GraphPad Prism 6, ANOVA with Bonferroni posttest, or Kruskal–Wallis test with Dunn's comparison was applied to all in vitro data. For in vivo allograft studies, we used SAS version 9.4 to test the overall differences in median tumor weight and median fold change in flux after 14 days treatment among the 4 cohorts (vehicle treatment served as the control). Nonparametric ANOVA with Bonferroni adjustments were used to adjust for small group sample sizes and non-normal distributions. The ANOVA for the median tumor weight and median fold change in flux indicated the overall significance differences. We tested 1-tailed hypothesis of improvements. For the *P0-SCH-Δ(39–121)-27* NF2 mouse model, 2-tailed unpaired Student's *t*-test was used to compare tumor burden and sizes in the trametinib- and vehicle-treated groups.

Results

We screened selumetinib, trametinib, PD0325901, MEK162, cobimetinib, and refametinib for effectiveness in reducing viability of 9 WT and MD-MSC/HSC lines after 48-hour (mouse) and 72-hour (human) treatments. Based upon 50% inhibitory concentration (IC_{50}) values, the inhibitors were overall more effective in MSCs compared with HSCs. Maximum loss of cell viability at 10 μM observed for all inhibitors tested was ~90–95% in MD-MSCs, compared with ~60% in MD-HSCs (Fig. 1A–B). The lowest inhibitor concentration tested produced a 20–40% reduction in MD-MSC viability. MEK inhibitors promoted a dose-dependent decrease in incorporation of 5-ethynyl-2'-deoxyuridine in both MD-MSC and MD-HSC (Supplementary Fig. 1). All 6 MEK inhibitors also exhibited less selectivity between WT- and MD-HSCs compared with MSC lines (2–5 fold compared with 6–15 fold; Fig. 1A–B and Supplementary Fig. 2).

Trametinib, PD0325901, and cobimetinib were further evaluated in vitro and in an allograft mouse model because each reduced viability of both MD-MSCs and MD-HSCs with submicromolar IC_{50} values and had some selectivity in HSCs. Each drug decreased phosphorylated pERK levels in MD-MSCs at 5 and 24 hours of treatment (Fig. 2A–B, Supplementary Fig. 3). Trametinib was the most potent, as pERK was not detected in the 0.001 μM sample. Among these 3 MEK1/2 inhibitors, cobimetinib was the least effective, based on sustained reduction of pERK levels over 24 hours. Higher cobimetinib concentrations (0.3–1 μM) were required to achieve an equivalent pERK reduction observed with 0.001 μM trametinib and PD0325901. As reported in other cell types, MEK inhibition is associated with a compensatory increase in pMEK levels (Fig. 2A–B, Supplementary Fig. 3).[35] In MD-MSCs, a more robust increase in pMEK levels was observed in cells treated with cobimetinib at 5 hours and PD0325901 at 24 hours. Because trametinib uniquely blocks Raf-dependent MEK phosphorylation,[14] the lowest increase in pMEK was observed in trametinib-treated cells. MD-HSCs also exhibited decreased pERK and increased pMEK following MEK inhibition, but at higher drug concentrations compared with MD-MSCs (Supplementary Fig. 4).

An examination of downstream MEK/ERK effectors in MD-MSCs treated with these inhibitors revealed decreased levels of cyclin D1, and increased $p27^{kip1}$ and cleaved caspase 3 levels (Fig. 2C–D). Membrane asymmetry assays confirmed an increase in apoptotic cell populations from ~2% in DMSO-treated to 20% and 45% in trametinib- and cobimetinib-treated MD-MSCs, respectively (Fig. 2E, Supplementary Fig. 4).

A proteomic analysis of trametinib-treated MD-MSCs was conducted to assess global changes in protein expression. The results were consistent with effective inhibition of MEK1/2 and downstream effectors and induction of apoptotic pathways. Trametinib-treated MD-MSCs had reduced expression of Ras/Raf/MEK/ERK pathway effectors including cyclin D1 and c-Myc and increased expression of pro-apoptotic proteins such as Bcl-2 interacting protein 3 like (BNIP3L) at 24 hours, compared with DMSO control (Fig. 3A). Ingenuity Pathway Analysis identified upstream regulators whose

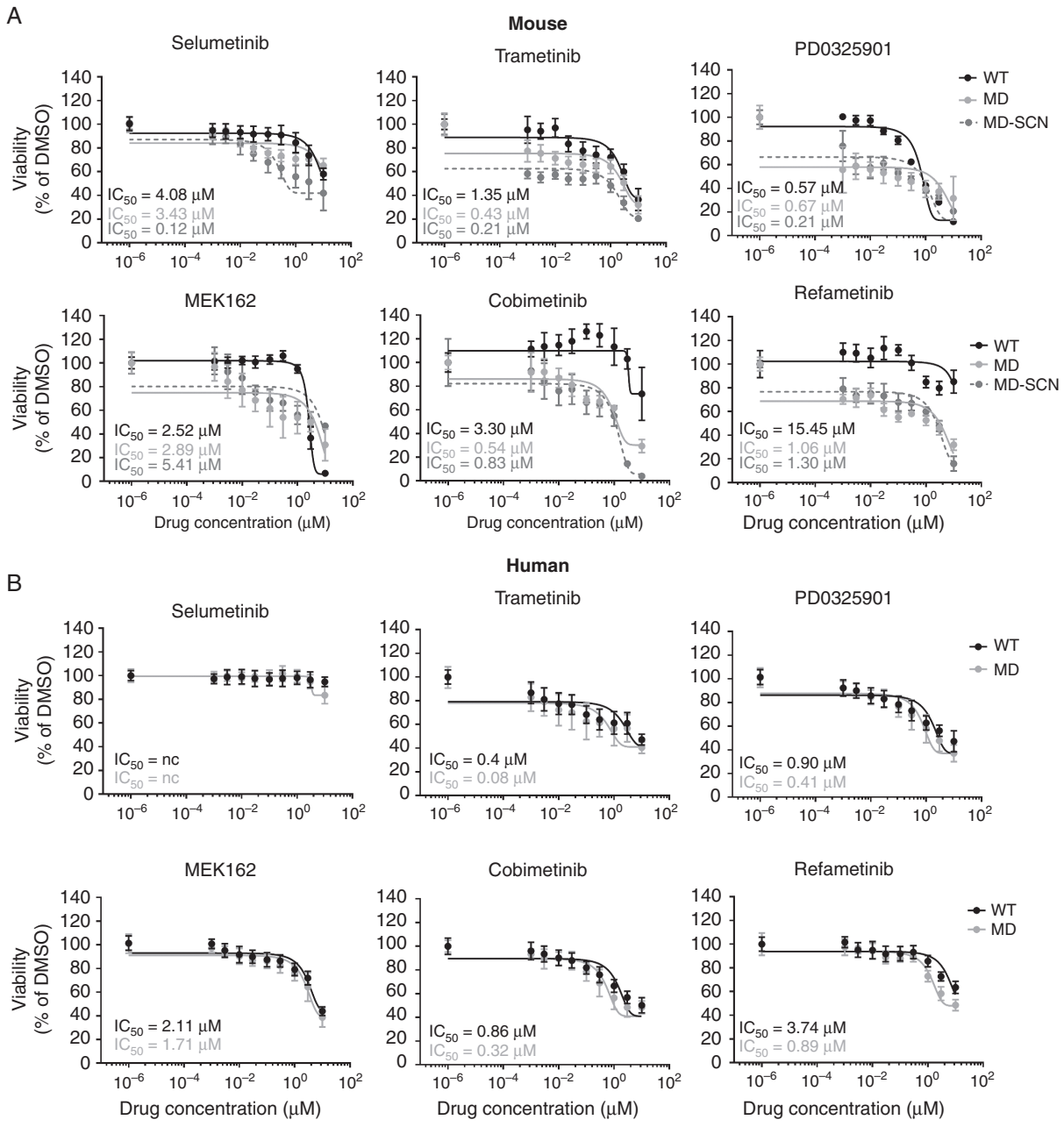

Fig. 1 MEK inhibitors reduce MD-MSC and MD-HSC viability. Screen of 6 MEK inhibitors against (A) mouse and (B) human WT and MD-SC lines treated for 48–72 h. Mean viability is plotted with IC_{50} values (n = 1–3 independent experiments; 8 replicates each).

modulation is consistent with the observed changes in protein levels. These included transforming growth factor beta (TGFβ), specificity protein 1, and p53 levels, whose levels were higher in trametinib-treated MD-MSCs compared with DMSO-treated controls (Fig. 3B–D).

To assess in vivo efficacy, we employed an orthotopic allograft model by grafting luciferase-expressing MD-MSCs into the sciatic nerves of NSG mice. Pharmacokinetic studies revealed that trametinib and cobimetinib had long $t_{1/2}$ values (~8 h and 4.8 h, respectively) and their nerve/plasma ratios increased with time (Fig. 4A). Upon confirmation of successful grafting (Supplementary Fig. 5), mice were gavaged daily for 14 days with trametinib (1 mg/ kg), PD0325901 (1.5 mg/ kg), or cobimetinib (20 mg/kg). All 3 MEK inhibitors significantly reduced the median tumor weight by 60–70% and the median fold change in flux from 0 to 14 days

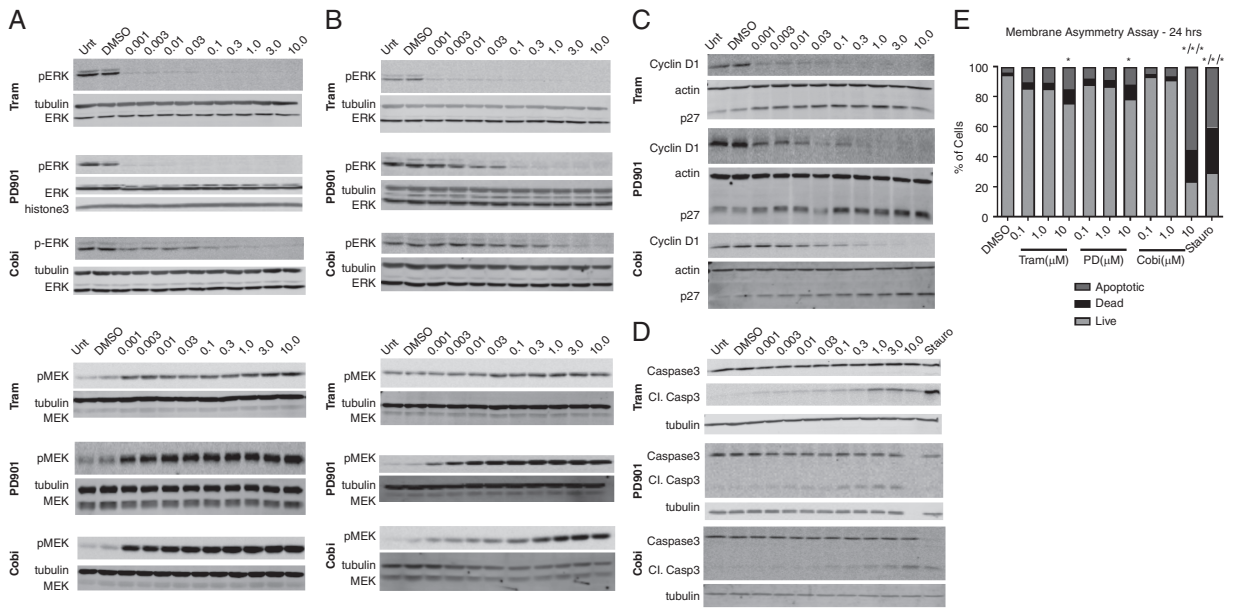

Fig. 2 MEK inhibitors promote G1 arrest and caspase-dependent apoptosis of MD-MSC in vitro. pERK1/2, pMEK1/2, cyclin D1, p27, and caspase-3 western blots of MD-MSC treated as indicated for (A) 5 h and (B-D) 24 h. All western blots are representative of 3–5 independent experiments. (E) Quantitation of membrane asymmetry assay of MD-MSC treated for 20 h with MEK inhibitors. Staurosporine (0.1 μM) served as a positive control for apoptosis ($n = 3$ independent experiments, 2-way ANOVA, $^*P < 0.05$).

by at least 80% compared with controls (Fig. 4B–D, Supplementary Fig. 6). Immunohistochemical analysis revealed that PD0325901 and cobimetinib were superior to trametinib in reducing pERK levels compared with the vehicle-treated group (Fig. 4E). Additionally, both inhibitors caused a more robust decrease in Ki-67 and cyclin D1 than trametinib, suggesting they were more potent inhibitors of graft growth in vivo. None of the inhibitors produced detectable caspase 3 cleavage nor did they affect vascularity as evidenced by CD31 staining (Fig. 4E).

Because trametinib is a well-tolerated FDA-approved drug and outperformed cobimetinib in cell assays, we assessed its efficacy in an 8-week study using the *P0-SCH-Δ(39–121)-27 NF2* schwannoma mouse model.[31,32] In this GEM model, trametinib efficacy was assessed by comparing the tumor burden, as defined by the percentage of tumor area versus total spinal nerve root area. Overall, trametinib promoted a 25% reduction in tumor burden ($P < 0.0001$) and a 37% decrease of average tumor size ($P = 0.0023$) (Fig. 5). Phosphorylated ERK immunohistochemistry of tumor samples revealed equivalent staining in trametinib- and vehicle-treated mice (data not shown), consistent with the allograft findings.

To examine the effect of MEK inhibition on human VS cells, primary cultures from 7 VS tumors were prepared and treated with PD0325901 or trametinib. All 7 VS tumors demonstrated ≥1 mutation in the *NF2* gene (Supplementary Table 1) and varying degrees of MEK1/2, pMEK, and pERK expression (Fig. 6A–B). Compared with DMSO-treated cells, trametinib (3 μM) moderately reduced cell viability of 2 of 7 VS, whereas PD0325901 (3 μM) reduced cell viability of 5 of the 7 VS tested (Fig. 6C–D). No significant correlations between viabilities and MEK1/2 and pMEK protein expression levels were identified, suggesting that drug response was independent of MEK expression.

To assess whether aberrant DNA methylation of the genome was associated with a lack of drug response, we compared methylation profiles of 2 VS with no response to PD0325901 tumors (VS27 and VS32) to the remaining 5 PD0325901-responsive tumors. In an unbiased evaluation, we identified 17 299 single cytosine-phosphate-guanine (CpG) sites with significantly different methylation levels ($P < 0.05$) between the drug responsive and nonresponsive VS. Among significant CpG sites, 4773 were hypermethylated (covering 3090 genes) and 12 526 were hypomethylated (covering 8051 genes) in the PD0325901-resistant compared with drug-sensitive VS. Supplementary Table 2 displays the top 20 hypermethylated and hypomethylated genes between the 2 groups. However, when false discovery rate (FDR) <0.05 was applied, *ELMOD1* (NM_001130037; Engulfment and cell motility domain 1) was the only gene that contained a CpG site (cg22355889) in the promoter region that was significantly hypermethylated in the PD0325901 nonresponsive VS.

Neighboring CpG sites often display closely related methylation patterns. To account for spatial correlations, we identified 34 differentially methylated regions (DMRs) with at least 5 consecutive

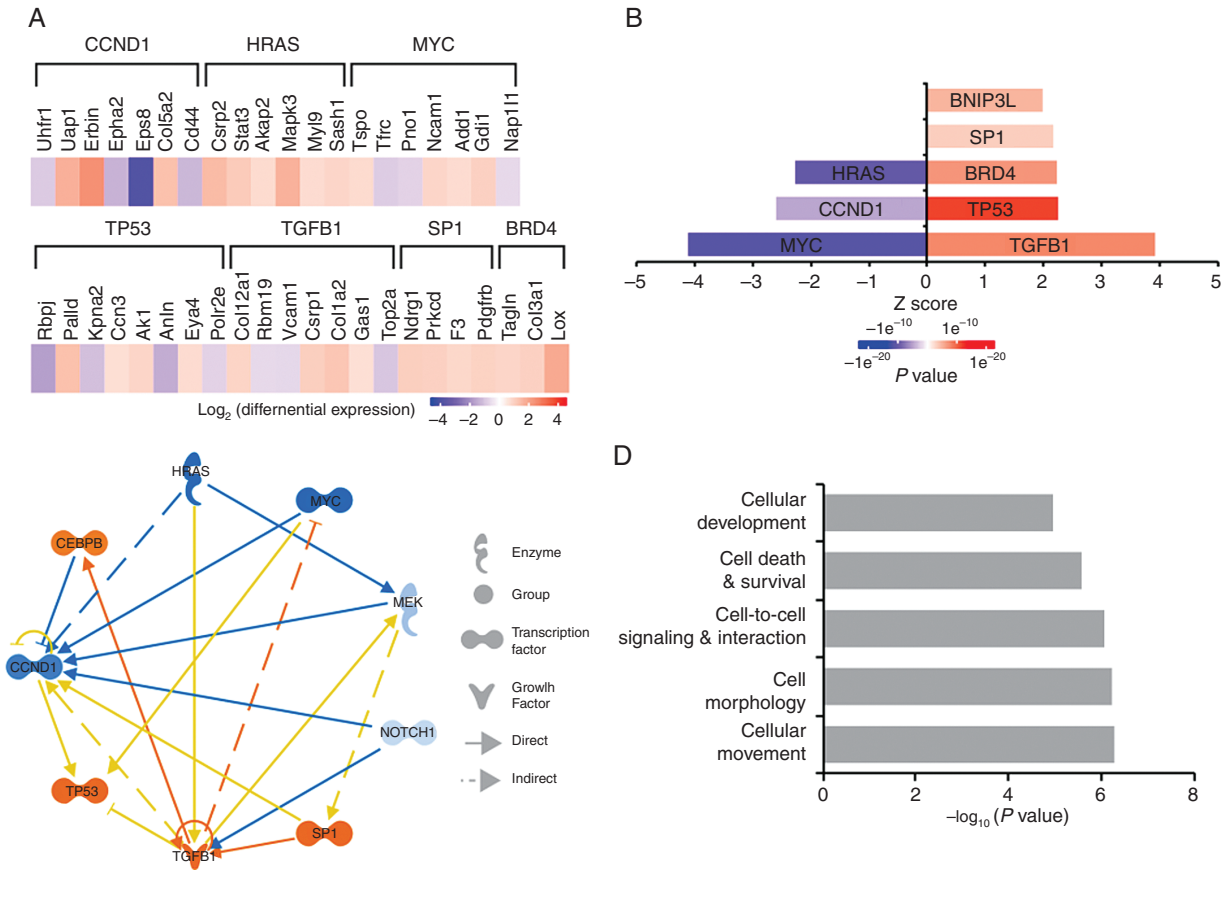

Fig. 3 Trametinib reduces signaling through Ras, Myc, and cyclin D1, and increases signaling through TP53 and TGFβ1. (A) Proteomic heat map showing differences in protein abundance in trametinib- versus DMSO-treated cells as determined by LC-MS/MS (blue: decreased expression, red: increased expression). (B) Predictions of upstream signaling pathways modulated by trametinib treatment. (C) Focus molecules and their connectivity based on Ingenuity Pathway Analysis of differentially expressed proteins in trametinib-treated versus DMSO-treated MD-MSC. (D) Differentially expressed proteins function in the indicated cellular processes ($n = 5$ replicate experiments).

hypermethylated or hypomethylated CpG loci in the PD0325901-nonresponsive compared with responsive VS (Supplementary Table 3). When examining individual DMRs, PD0325901 nonresponsive VS had DMRs in genes involved in non-MEK merlin signaling, including the *ATF6B* (activating transcription factor 6) and RXR (retinoid x receptor) genes associated with the phosphoinositide 3-kinase (PI3K/Akt) pathway and ATP6V1C1 (V-type proton ATPase subunit C1) of the mammalian target of rapamycin pathway. Gene ontology pathway analysis revealed no significant enrichment pathways for DMRs. However, when using a targeted approach assessing genes associated with merlin signaling, cancer, drug resistance, cell death, and survival, additional DMRs were identified. ARCHS4 pathway analysis revealed significant enrichment in epidermal growth factor receptor and tumor suppressor RPS6KA2 (ribosomal protein S6 kinase A2) human kinase pathways (http://amp.pharm.mssm.edu/Enrichr/. Accessed January 20, 2019).

Discussion

NF2 is a genetic disorder involving the development of multiple nervous system tumors that each impact neurological functions. Individuals affected by NF2 develop bilateral VS that cause severe hearing loss, disabling imbalance, and even life-threatening hydrocephalus from brainstem and cerebellar compression. Observation of tumor growth rate and hearing is standard as enthusiasm for microsurgical resection in NF2 is low due to consequential and irreversible limitations on nerve function and quality of life.[8] In the same respect, the long-term sequelae of utilizing radiotherapy is not so uncommon to disregard the risk of developing malignant transformation of benign tumors.[5–7,9,10] Off-label use of select FDA-approved chemotherapeutic agents for NF2 in clinical trials show moderate tumor control at best and hearing stabilization in only some NF2 patients.[36–41] However, even small effects

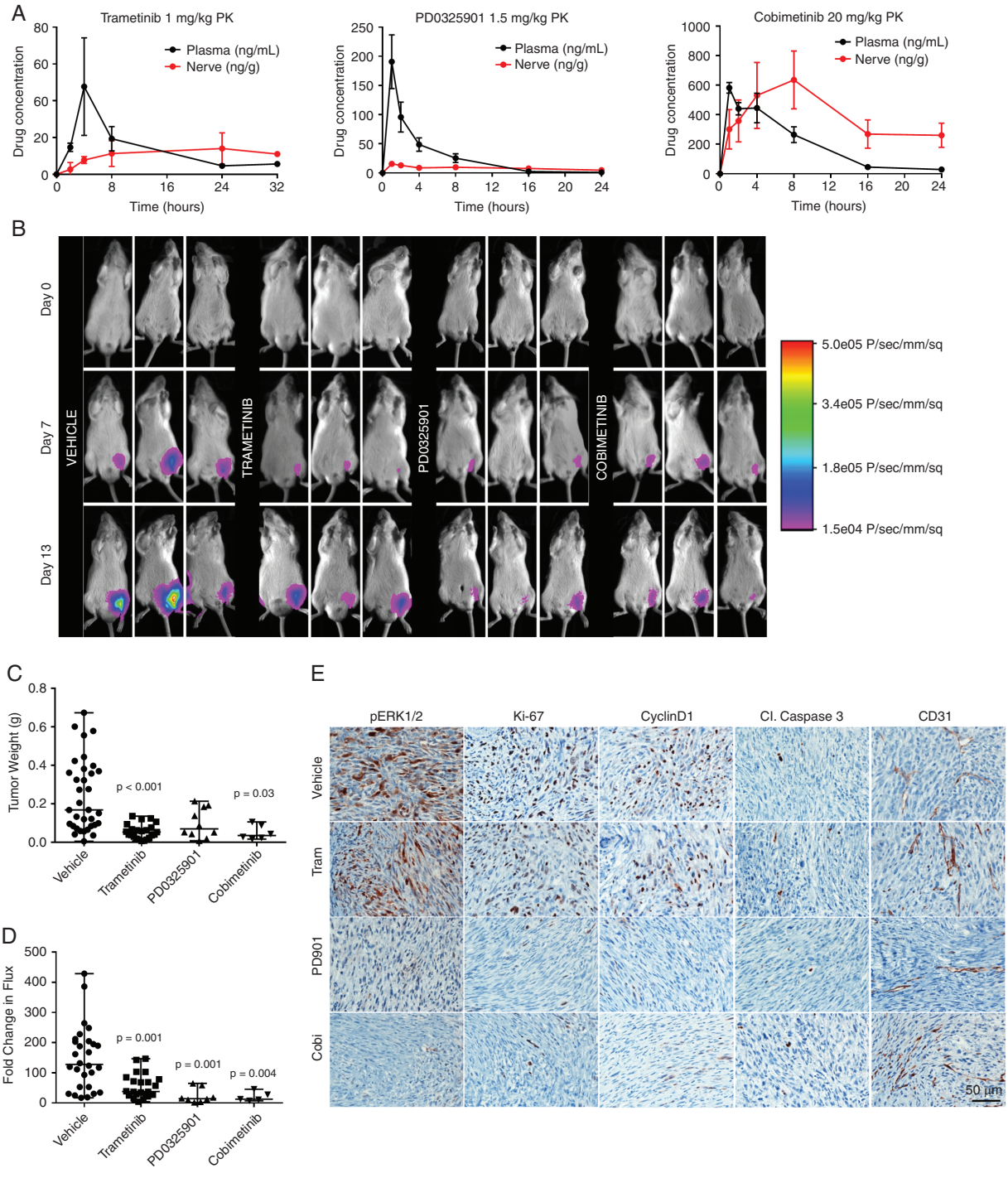

Fig. 4 MEK inhibitors slow MD-MSC growth in NSG mice. (A) Pharmacokinetic analysis for plasma and nerve following a single drug dose. (B) Representative bioluminescent (BL) images for indicated times. (C) Median tumor weights after 14 days of drug treatment compared with vehicle ($n = 6$–35 mice, nonparametric ANOVA). (D) BL signals were normalized to day 0 for each mouse and fold change in flux (photons/sec) after 14 days of treatment is shown (nonparametric ANOVA, median values shown). (E) Representative graft immunohistochemistry images for pERK1/2, Ki-67, cyclin D1, cleaved caspase 3, and CD31.

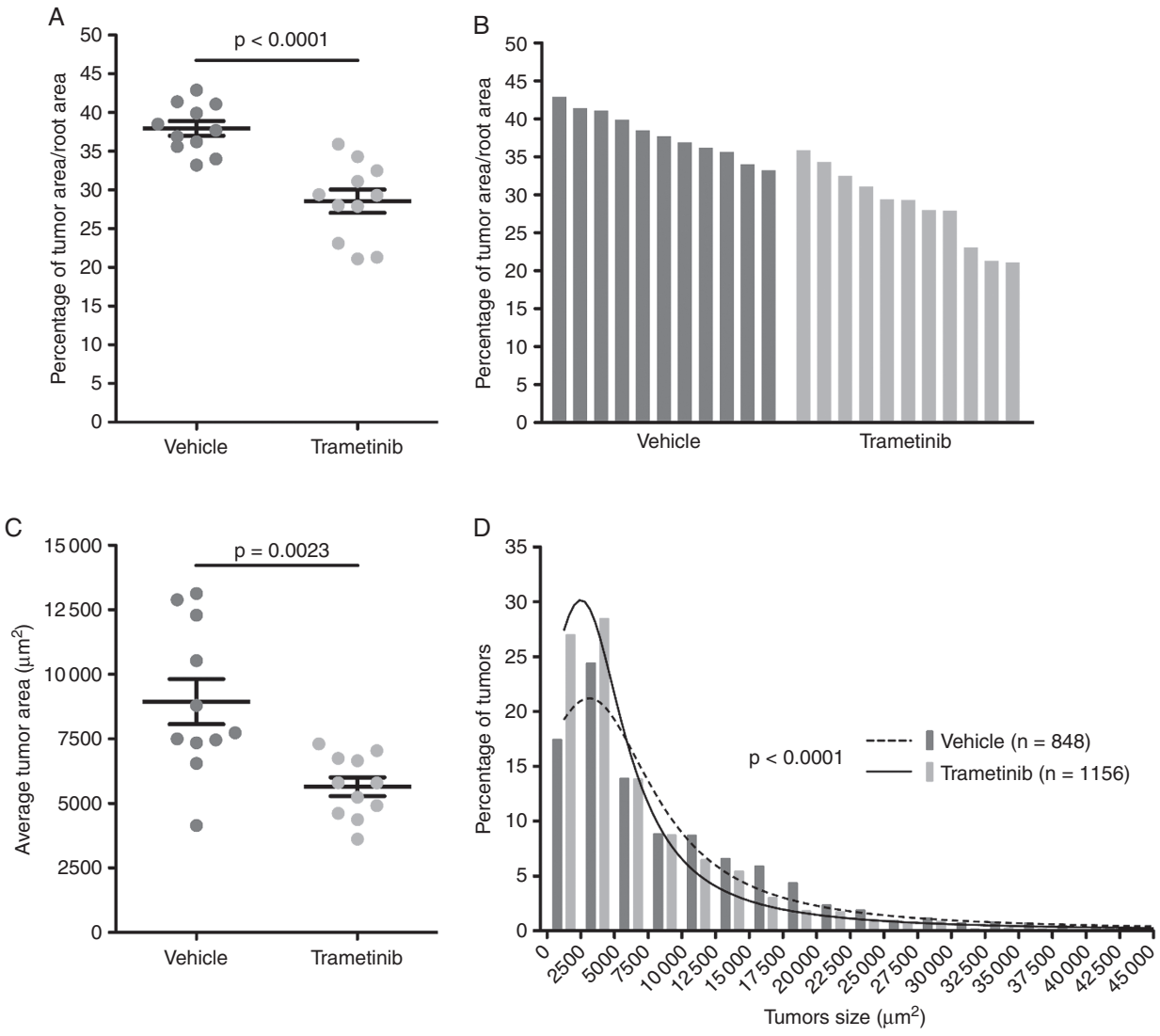

Fig. 5 Trametinib reduces schwannoma growth in the *P0-SCH-Δ(39–121)-27* NF2 mouse model. *P0-SCH-Δ(39–121)-27* mice were treated daily with trametinib (1 mg/kg, p.o., 7 d/wk) for 8 weeks starting at 4 weeks of age. (A) Reduction by 25% of the average tumor burden, calculated as percentage of tumor area versus total spinal nerve root area for trametinib-treated mice ($n = 11$) compared with vehicle-treated mice ($n = 11$). (B) Waterfall plot showing tumor burden for each vehicle- and trametinib-treated mouse. (C) Treatment with trametinib reduced average tumor size by 37% in trametinib-treated compared with vehicle-treated mice. (D) Histogram of tumor size distribution demonstrated a significantly higher percentage of smaller tumors in trametinib-treated ($n = 1156$ tumors) compared with vehicle-treated ($n = 848$ tumors) mice.

can impact survival and quality of life in individual NF2 patients. Therefore, the discovery of effective NF2 drug therapies is critical.

Currently, 2 clinical trials are enrolling pediatric NF2 patients to test effectiveness of selumetinib and cobimetinib in reducing tumor volume and preserving hearing (NCT03095248 and NCT02639546). However, the preclinical efficacies for selumetinib and cobimetinib have not been established. These trials are supported by knowledge that merlin loss is associated with increased mitogen-activated protein kinase signaling, and[42] success of selumetinib in shrinking plexiform neurofibromas in NF1 children.[15] Our study is the first to evaluate a panel of MEK inhibitors in mouse and human NF2 schwannoma models.

Of the 6 inhibitors screened against multiple mouse and human SC lines, trametinib, PD0325901, and cobimetinib reduced MD-SC viability at submicromolar IC_{50} values and were the most effective in non-immortalized human MD-SCs (Fig. 1A). Notably, selumetinib was the least effective in MD-HSCs and was not a top performer in MD-MSCs (based on maximum effect and IC_{50} values). In vitro, trametinib, PD0325901, and cobimetinib reduced pERK levels, modulated cyclin D1 and p27 levels in a manner consistent with a G_1/S cell cycle arrest, and induced caspase-dependent apoptosis in MD-MSCs. The proteomic study conducted in

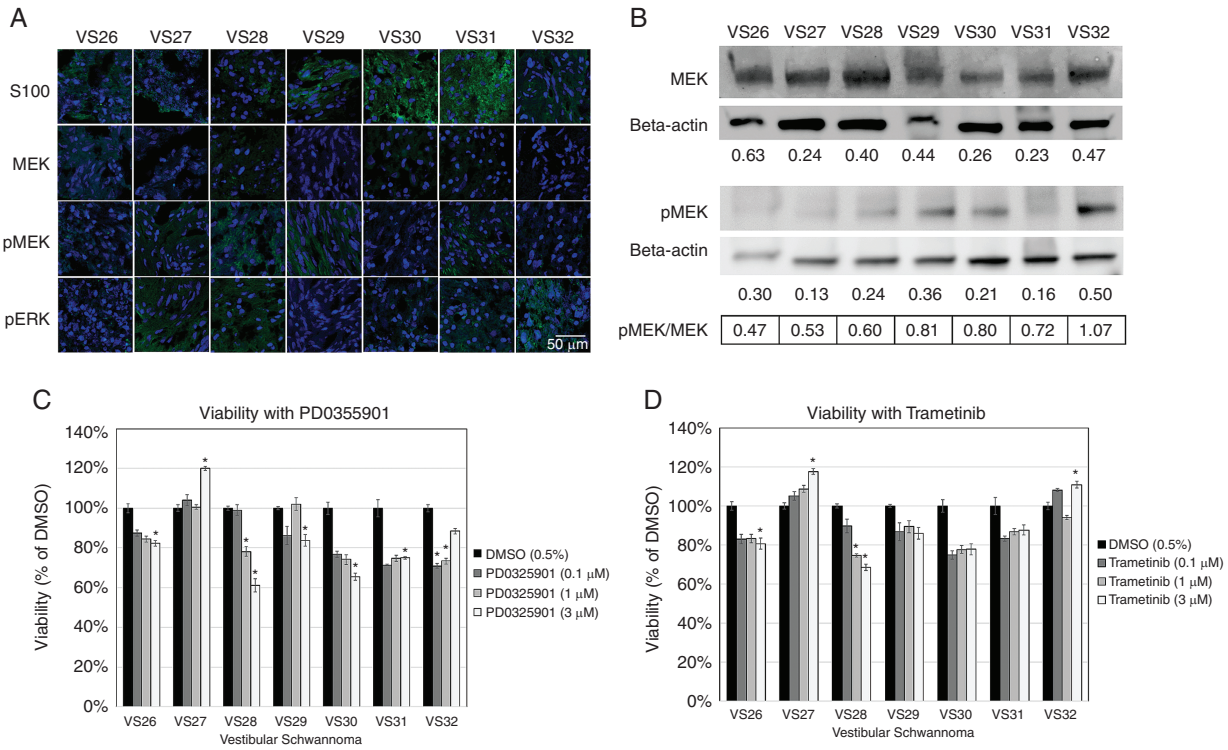

Fig. 6 MEK inhibitors reduce viability of a subset of primary human VS cells. (A) Immunohistochemistry shows S100 positivity and variable expression levels of MEK, pMEK, and pERK (green) in VS tumors (4′,6′-diamidino-2-phenylindole nuclear stain, blue). (B) Western blots demonstrate expression of MEK and pMEK for VS with beta-actin as the standard. Relative expression levels of MEK and pMEK were displayed and expressed as a ratio of pMEK/MEK. (C–D) Cell viability assays for PD0325901 and trametinib were performed and viability was normalized to 0.5% DMSO controls.

trametinib-treated MD-MSC further corroborated this conclusion by revealing decreased signaling in the Ras-ERK-cyclin D1 pathway and increased signaling from BNIP3L, a pro-apoptotic subfamily in the Bcl-2 family of proteins.

We used 2 in vivo models to evaluate drug efficacy: a 2-week treatment protocol aimed at slowing growth of established MD-MSCs nerve grafts in NSG mice, and an 8-week chemoprevention protocol aimed at preventing appearance of schwannomas in a GEM model. In the nerve grafts, PD0325901 and cobimetinib produced a stronger reduction in MD-MSC growth compared with trametinib, likely from persistent inhibition of pERK, cyclin D1, and Ki-67 levels.Trametinib did not significantly decrease pERK, cyclin D1 and Ki-67 levels in allografts at the study endpoint when compared with vehicle-treated controls, supporting the conclusion that cells in the allografts were developing resistance to trametinib. Similar responses to trametinib were obtained with the GEM model. Although the number and size of schwannomas were reduced in the GEM model following 8 weeks of trametinib treatment, immunohistochemically, pERK levels in trametinib-treated schwannomas were equivalent to controls. An adaptive response to trametinib has been reported in triple-negative breast cancer.[43] Trametinib treatment resulted in degradation of c-Myc and in assembly of bromodomain containing 4 (BRD4)-containing transcriptional enhancers on promoters of adaptive response genes, resulting in activation of compensatory pathways associated with drug resistance.[43] Our proteomic analysis similarly revealed decreased c-Myc levels and increased BRD4 levels in MD-MSCs treated with trametinib (Fig. 3). BRD4 in trametinib-induced adaptive response promoter complexes can be displaced by treatment with bromodomain and extraterminal domain family (BET) bromodomain inhibitors.[44] A study of BET bromodomain inhibitors in ovarian cancer revealed reduced activation of ERK, Akt, and Src kinase following treatment, suggesting that these pathways may be activated by bromodomain-containing transcriptional enhancers.[45] Additionally, BET family bromodomains were involved in reactivation of the Src/focal adhesion kinase pathway in breast cancer cells following inhibition of ErbB2 with lapatinib.[46] Collectively, these studies suggest that trametinib treatment may promote assembly of BRD-containing transcriptional enhancers that can activate compensatory proliferative pathways. Future studies examining the effects of bromodomain and Src inhibitors in combination with MEK inhibitors are warranted.

Of the 7 primary human VS cultures tested, only a subset responded to either PD0325901 or trametinib by reducing cell viability by 15–40% of controls. Although the trend of response to both drugs was similar within individual VS cultures, the differing response rate to the drugs was

71% versus 29%, respectively, and did not correlate with baseline MEK or pMEK expression (Fig. 6A–D). The differing response rate can be attributed to the 10-fold higher potency of cobimetinib compared with PD0325901 (Fig. 6C–D).[18,19] VS cells also demonstrated a large variety of *NF2* mutations, which can have differential effects on merlin-dependent cell proliferation and survival pathways. Methylome exploration identified *ELMOD1* as the single gene with a hypermethylated promoter and an FDR <0.05 in nonresponsive VS compared with responsive VS. ELMOD1 is a GTPase activator for small GTPases in the ADP ribosylation factor (Arf) and Arf-like families (Arl2). In PD0325901 nonresponsive VS, a hypermethylated promoter in *ELMOD1* is expected to reduce ELMOD1 expression, increase Arl2 activity, and alter normal microtubule dynamics.[47] This may allow VS cells to circumvent traditional mechanisms of cell cycle arrest and cell death.[47] Further investigation into how tumor heterogeneity in NF2 contributes to drug resistance and disease progression is imperative for identifying treatment modalities to overcome resistance to MEK inhibition.

We present a comprehensive preclinical analysis of MEK inhibitors in mouse and human NF2 schwannoma models and primary human VS. Although differences in response were observed between drugs, species, and models, our cumulative results support MEK inhibitors for the treatment of a subset of NF2 schwannomas. We demonstrate that differences in treatment response to MEK inhibitors depends on genetic and epigenetic differences between tumors that can impact downstream merlin signaling, drug resistance mechanisms, and adaptive pathways to evade cell death or arrest. By understanding the mechanisms of drug response and resistance to MEK inhibitors in individual tumors, we can identify optimal combination therapies to maximize tumor control, determine important genetic and molecular biomarkers to predict patient outcomes, and develop precision medicine algorithms for NF2 treatment.

Supplementary Material

Supplementary data are available at *Neuro-Oncology* online.

Keywords

merlin tumor suppressor | methylome | NF2 transgenic mice | MEK inhibitors | patient-derived vestibular schwannomas

Funding

This work was supported by Department of Defense Congressionally Directed Medical Research Program (W81XWH-15-1-0446 to CFV and W81XWH-16-1-0104 to LSC), National Institutes of Health/National Institute on Deafness and Other Communication Disorders (R0-DC005575 and R01-DC012115 to XZL), and the Children's Tumor Foundation with contracts to CFV and MAF.

Acknowledgments

We thank Drs Jacques Morcos and Michael Ivan for their efforts harvesting human VS tumors and patients for donated tumor samples. We acknowledge Anthony Griswold, PhD, Division Head of the Center for Genetic Epidemiology and Statistical Genetics at the University of Miami Miller School of Medicine, for bioinformatics and statistical analysis of DNA methylation experiments.

Conflict of interest statement. CFV is a named inventor on unrelated patents. MG and JV receive research funding from Recursion Pharmaceuticals. Other authors report that no conflicts of interest exist.

Authorship statement. *Designed experiments*: CFV, MCF, MAF, JV, MG, JK and CTD. *Supervised work:* CFV, CTD, MG, HM, and LSC. *Cell and allograft studies*: MAF, SKP, JN, KB, AP, MCF. *Human VS work*: CTD, OB, RM, DY, XL, FT, JIY. *GEM model*: MG, JV. *Proteome analysis*: AC, JK, TM, HM. *Histology*: LSC, RS, JH. *Flow cytometry analysis*: AJC. *Statistical analysis*: JNS. CFV, MAF and LSC wrote the initial draft and all authors edited the manuscript.

Portions of Figs. 1, 3, and 5 were presented at the annual Neurofibromatosis Conference in Washington DC in June 2017.

References

1. Rouleau GA, Merel P, Lutchman M, et al. Alteration in a new gene encoding a putative membrane-organizing protein causes neuro-fibromatosis type 2. *Nature*. 1993;363(6429):515–521.
2. Trofatter JA, MacCollin MM, Rutter JL, et al. A novel moesin-, ezrin-, radixin-like gene is a candidate for the neurofibromatosis 2 tumor suppressor. *Cell*. 1993;72(5):791–800.
3. Evans DG. Neurofibromatosis type 2 (NF2): a clinical and molecular review. *Orphanet J Rare Dis*. 2009;4:16.
4. Blakeley JO, Evans DG, Adler J, et al. Consensus recommendations for current treatments and accelerating clinical trials for patients with neurofibromatosis type 2. *Am J Med Genet A*. 2012;158A(1):24–41.
5. Chung LK, Nguyen TP, Sheppard JP, et al. A systematic review of radiosurgery versus surgery for neurofibromatosis type 2 vestibular schwannomas. *World Neurosurg*. 2018;109:47–58.
6. Evans DG, Birch JM, Ramsden RT, Sharif S, Baser ME. Malignant transformation and new primary tumours after therapeutic radiation for benign disease: substantial risks in certain tumour prone syndromes. *J Med Genet*. 2006;43(4):289–294.
7. Kim BS, Seol HJ, Lee JI, et al. Clinical outcome of neurofibromatosis type 2-related vestibular schwannoma: treatment strategies and challenges. *Neurosurg Rev*. 2016;39(4):643–653.

8. Nowak A, Dziedzic T, Czernicki T, et al. Strategy for the surgical treatment of vestibular schwannomas in patients with neurofibromatosis type 2. *Neurol Neurochir Pol*. 2015;49(5):295–301.
9. Seferis C, Torrens M, Paraskevopoulou C, Psichidis G. Malignant transformation in vestibular schwannoma: report of a single case, literature search, and debate. *J Neurosurg*. 2014;121(Suppl):160–166.
10. Sun S, Liu A. Long-term follow-up studies of Gamma Knife surgery for patients with neurofibromatosis type 2. *J Neurosurg*. 2014;121(Suppl):143–149.
11. Hilton DA, Ristic N, Hanemann CO. Activation of ERK, AKT and JNK signalling pathways in human schwannomas in situ. *Histopathology*. 2009;55(6):744–749.
12. Morrison H, Sperka T, Manent J, Giovannini M, Ponta H, Herrlich P. Merlin/neurofibromatosis type 2 suppresses growth by inhibiting the activation of Ras and Rac. *Cancer Res*. 2007;67(2):520–527.
13. Petrilli AM, Fernández-Valle C. Role of merlin/NF2 inactivation in tumor biology. *Oncogene*. 2016;35(5):537–548.
14. McDermott L, Qin C. Allosteric MEK1/2 inhibitors for the treatment of cancer: an overview. *J Drug Res Dev*. 2015;1:1–9. doi: 10.16966/jdrd.101.
15. Dombi E, Baldwin A, Marcus LJ, et al. Activity of selumetinib in neurofibromatosis type 1–related plexiform neurofibromas. *N Engl J Med*. 2016;375(26):2550–2560.
16. Ammoun S, Schmid MC, Ristic N, et al. The role of insulin-like growth factors signaling in merlin-deficient human schwannomas. *Glia*. 2012;60(11):1721–1733.
17. Ammoun S, Schmid MC, Triner J, Manley P, Hanemann CO. Nilotinib alone or in combination with selumetinib is a drug candidate for neurofibromatosis type 2. *Neuro Oncol*. 2011;13(7):759–766.
18. Yamaguchi T, Kakefuda R, Tajima N, Sowa Y, Sakai T. Antitumor activities of JTP-74057 (GSK1120212), a novel MEK1/2 inhibitor, on colorectal cancer cell lines in vitro and in vivo. *Int J Oncol*. 2011;39(1):23–31.
19. Barrett SD, Bridges AJ, Dudley DT, et al. The discovery of the benzhydroxamate MEK inhibitors CI-1040 and PD 0325901. *Bioorg Med Chem Lett*. 2008;18(24):6501–6504.
20. Jessen WJ, Miller SJ, Jousma E, et al. MEK inhibition exhibits efficacy in human and mouse neurofibromatosis tumors. *J Clin Invest*. 2013;123(1):340–347.
21. Jousma E, Rizvi TA, Wu J, et al. Preclinical assessments of the MEK inhibitor PD-0325901 in a mouse model of Neurofibromatosis type 1. *Pediatr Blood Cancer*. 2015;62(10):1709–1716.
22. Signorelli J, Shah Gandhi A. Cobimetinib. *Ann Pharmacother*. 2017;51(2):146–153.
23. Wong H, Vernillet L, Peterson A, et al. Bridging the gap between preclinical and clinical studies using pharmacokinetic-pharmacodynamic modeling: an analysis of GDC-0973, a MEK inhibitor. *Clin Cancer Res*. 2012;18(11):3090–3099.
24. Choo EF, Ng CM, Berry L, et al. PK-PD modeling of combination efficacy effect from administration of the MEK inhibitor GDC-0973 and PI3K inhibitor GDC-0941 in A2058 xenografts. *Cancer Chemother Pharmacol*. 2013;71(1):133–143.
25. Hoeflich KP, Merchant M, Orr C, et al. Intermittent administration of MEK inhibitor GDC-0973 plus PI3K inhibitor GDC-0941 triggers robust apoptosis and tumor growth inhibition. *Cancer Res*. 2012;72(1):210–219.
26. Rice KD, Aay N, Anand NK, et al. Novel carboxamide-based allosteric MEK inhibitors: discovery and optimization efforts toward XL518 (GDC-0973). *ACS Med Chem Lett*. 2012;3(5):416–421.
27. Rosen LS, LoRusso P, Ma WW, et al. A first-in-human phase I study to evaluate the MEK1/2 inhibitor, cobimetinib, administered daily in patients with advanced solid tumors. *Invest New Drugs*. 2016;34(5):604–613.
28. Petrilli AM, Fuse MA, Donnan MS, et al. A chemical biology approach identified PI3K as a potential therapeutic target for neurofibromatosis type 2. *Am J Transl Res*. 2014;6(5):471–493.
29. Fuse MA, Plati SK, Burns SS, et al. Combination therapy with c-Met and Src inhibitors induces caspase-dependent apoptosis of merlin-deficient schwann cells and suppresses growth of schwannoma cells. *Mol Cancer Ther*. 2017;16(11):2387–2398.
30. Petrilli AM, Garcia J, Bott M, et al. Ponatinib promotes a G1 cell-cycle arrest of merlin/NF2-deficient human schwann cells. *Oncotarget*. 2017;8(19):31666–31681.
31. Giovannini M, Robanus-Maandag E, Niwa-Kawakita M, et al. Schwann cell hyperplasia and tumors in transgenic mice expressing a naturally occurring mutant NF2 protein. *Genes Dev*. 1999;13(8):978–986.
32. Giovannini M, Bonne NX, Vitte J, et al. mTORC1 inhibition delays growth of neurofibromatosis type 2 schwannoma. *Neuro Oncol*. 2014;16(4):493–504.
33. Cox J, Neuhauser N, Michalski A, Scheltema RA, Olsen JV, Mann M. Andromeda: a peptide search engine integrated into the MaxQuant environment. *J Proteome Res*. 2011;10(4):1794–1805.
34. Smyth GK, Michaud J, Scott HS. Use of within-array replicate spots for assessing differential expression in microarray experiments. *Bioinformatics*. 2005;21(9):2067–2075.
35. Gilmartin AG, Bleam MR, Groy A, et al. GSK1120212 (JTP-74057) is an inhibitor of MEK activity and activation with favorable pharmacokinetic properties for sustained in vivo pathway inhibition. *Clin Cancer Res*. 2011;17(5):989–1000.
36. Blakeley JO, Plotkin SR. Therapeutic advances for the tumors associated with neurofibromatosis type 1, type 2, and schwannomatosis. *Neuro Oncol*. 2016;18(5):624–638.
37. Goutagny S, Raymond E, Esposito-Farese M, et al. Phase II study of mTORC1 inhibition by everolimus in neurofibromatosis type 2 patients with growing vestibular schwannomas. *J Neurooncol*. 2015;122(2):313–320.
38. Karajannis MA, Legault G, Hagiwara M, et al. Phase II trial of lapatinib in adult and pediatric patients with neurofibromatosis type 2 and progressive vestibular schwannomas. *Neuro Oncol*. 2012;14(9):1163–1170.
39. Karajannis MA, Legault G, Hagiwara M, et al. Phase II study of everolimus in children and adults with neurofibromatosis type 2 and progressive vestibular schwannomas. *Neuro Oncol*. 2014;16(2):292–297.
40. Plotkin SR, Halpin C, McKenna MJ, Loeffler JS, Batchelor TT, Barker FG 2nd. Erlotinib for progressive vestibular schwannoma in neurofibromatosis 2 patients. *Otol Neurotol*. 2010;31(7):1135–1143.
41. Plotkin SR, Merker VL, Halpin C, et al. Bevacizumab for progressive vestibular schwannoma in neurofibromatosis type 2: a retrospective review of 31 patients. *Otol Neurotol*. 2012;33(6):1046–1052.
42. Yi C, Troutman S, Fera D, et al. A tight junction-associated merlin-angiomotin complex mediates merlin's regulation of mitogenic signaling and tumor suppressive functions. *Cancer Cell*. 2011;19(4):527–540.
43. Bevill SM, Zawistowski JS, Johnson GL. Enhancer remodeling regulates epigenetic adaptation and resistance to MEK1/2 inhibition in triple-negative breast cancer. *Mol Cell Oncol*. 2017;4(6):e1300622.
44. Zawistowski JS, Bevill SM, Goulet DR, et al. Enhancer remodeling during adaptive bypass to MEK inhibition is attenuated by pharmacologic targeting of the P-TEFb complex. *Cancer Discov*. 2017;7(3):302–321.
45. Kurimchak AM, Shelton C, Duncan KE, et al. Resistance to BET bromodomain inhibitors is mediated by kinome reprogramming in ovarian cancer. *Cell Rep*. 2016;16(5):1273–1286.
46. Stuhlmiller TJ, Miller SM, Zawistowski JS, et al. Inhibition of lapatinib-induced kinome reprogramming in ERBB2-positive breast cancer by targeting BET family bromodomains. *Cell Rep*. 2015;11(3):390–404.
47. Zhou C, Cunningham L, Marcus AI, Li Y, Kahn RA. Arl2 and Arl3 regulate different microtubule-dependent processes. *Mol Biol Cell*. 2006;17(5):2476–2487.